A comparison between a white LED confocal imaging system and a conventional flash fundus camera using chromaticity analysis

Valentina Sarao
University of Udine
Daniele Veritti
University of Udine
Enrico Borrelli
Doheny Eye Institute
SriniVas R Sadda
Doheny Eye Institute
Enea Poletti
Centervue SPA
Paolo Lanzetta (paolo.lanzetta@uniud.it)
Universita degli Studi di Udine

Research Article

Keywords: Chromaticity; Confocal white LED system; conventional flash fundus camera; Eidon; Topcon

Posted Date: January 15th, 2019

DOI: https://doi.org/10.21203/rs.2.226/v1

Version of Record: A version of this preprint was published on November 19th, 2019. See the published version at https://doi.org/10.1186/s12886-019-1241-8.

Abstract

BACKGROUND: Conventional flash fundus camera captures color images that are over-saturated in the red channel, producing a retinal picture that looks washed-out and uniform. A white LED confocal device was recently introduced to provide a neutral-looking retinal image. With this study we aimed to evaluate the color rendering properties of the white LED confocal system and to compare it to a conventional flash fundus camera through the use of chromaticity analysis.

METHODS: A fully automated white LED confocal device (Eidon, Centervue, Padova, Italy) was used to capture fundus images from healthy volunteers and patients with retinal diseases. The same pictures were acquired with a flash fundus camera (Triton, Topcon Corporation, Tokyo, Japan). All color images were evaluated with respect to the chromaticity. Color analysis was performed according to the image color signature. Color signature of an image was defined as the distribution of its pixels in the rgb chromaticity space. The descriptors used for the analysis are the average and variability of the barycenter positions, the average of the variability and the number of unique colors (NUC) of all signatures.

RESULTS: Two hundred thirty-three color fundus photographs were acquired with each retinal camera. The images acquired by confocal white LED device demonstrated an average barycenter position (rgb = [0.448, 0.328, 0.224]) closer to the center of the chromaticity space, while conventional fundus camera provides images with a clear shift toward red at the expense of the blue and green (rgb = [0.574, 0.278, 0.148] ($p<0.001$). The variability of the barycenter positions was higher in white LED confocal system than in conventional flash fundus camera. The average variability of the distributions was higher (0.003 ± 0.007, $p<0.001$) in the Eidon images compared to Topcon camera, indicating a greater richness of color. The NUC percentage was higher for white LED confocal device than for conventional flash fundus camera (0.071% versus 0.025%, $p<0.001$).

CONCLUSIONS: Confocal white LED system provides well-balanced color images with a wider richness of color content compared to conventional flash fundus camera. The overall higher chromaticity of Eidon device may provide benefits in terms of discriminative power and diagnostic accuracy.

KEYWORDS: Chromaticity; Confocal white LED system; conventional flash fundus camera; Eidon; Topcon.

Background

Color fundus photography is an important tool in the diagnosis and monitoring of various retinal diseases. Clear and detailed photographs allow for an accurate evaluation of the ocular fundus and provide a precise documentation of retinal findings that can be archived, shared for telemedicine applications, or used as a valuable educational tool.

Fundus photography dates back to the late 1800 when Jackman and Webster first described a technique for photographing the human retina [1]. In recent years, retina cameras have been optimised for non-

mydriatic image acquisition and have transitioned from analogue (i.e. film) to digital image capture [2,3]. In such devices, a bright flash is used to illuminate the ocular fundus, the light reflected is then captured on the pixel array of a charge-coupled device, and hence a digital image is generated. Conventional fundus cameras illuminate large areas of the retina, typically with a flash lamp, and capture 35-45 degrees high resolution digital images. Currently, color images acquired with traditional fundus camera continue to play a pivotal role in documentation, diagnosis and monitoring of retinal disorders. However, conventional flash devices frequently capture color images that are over-saturated in the red channel, yielding a retinal picture that often looks washed-out and uniform [4].

More recent fundus imaging systems have taken advantage of principles of confocal scanning laser ophthalmoscopy (cSLO). Instead of a flash, cSLO uses laser light to illuminate the retina. Images are obtained through point-by-point scanning of the entire retinal field by a focused laser beam, then capturing the reflected light through a small confocal pinhole, which, in turn, suppresses any scattered or reflected light outside the focal plane that could potentially blur the image. This results in a sharp, high-contrast image of an object layer located within the focal plane.

The advantages of using cSLO over traditional fundus photography include improved image quality, suppression of scattered light, patient comfort through less bright light, and better imaging of patients with poor dilation. However, as cSLO imaging utilises a laser light source at a specific wavelength, the use of a single light source only provides grayscale, and not color images. Therefore, there have been attempts to generate “pseudo-color” fundus images by combining lasers of different wavelengths. However, the resultant image is often unsatisfactory and the color rendition appears to differ from ophthalmoscopic examination with white light [5].

Recently, a non-mydriatic system that combines confocal technology with white Light Emitting Diode (LED) illumination has been introduced to provide a neutral-looking retinal image (Eidon (Centervue, Padova, Italy)) [6,7].

Color images acquired by traditional fundus camera and by this new, white LED, confocal device, however, may still differ in color rendering and may the differences in chromatic information could have implications for the detection and classification of pathological features associated with various eye diseases.

The aim of this work is to evaluate the color rendering of color fundus photographs acquired with the white LED light confocal system and to compare it to a conventional fundus camera through the use of chromaticity analysis.

Methods

Study Design

This is a prospective, observational, cross-sectional case series. The study protocol follows the tenets of the Declaration of Helsinki and was approved by the local review board. Written, informed consent was obtained from all the participants before entering the study.

Study population

Consecutive patients, aged 18 or over, were recruited and enrolled at the Istituto Europeo di Microchirurgia Oculare - IEMO (Udine, Italy) between September 2017 and December 2017. Patients were excluded from the study if they were unable to give informed consent, were unable to position at the slit lamp table, or were unable to fixate on the light target of the camera.

Study protocol

Each subject underwent a complete ophthalmologic examination, including best-corrected visual acuity (BCVA) assessment on standard Early Treatment Diabetic Retinopathy Study (ETDRS) charts, slit-lamp biomicroscopy, and dilated ophthalmoscopy. On the same day, non-mydriatic fundus images were acquired using a fully automated retinal imaging system (Eidon, Centervue, Padova, Italy) (system 1) and a conventional flash fundus camera (Topcon Corporation, Tokyo, Japan) (system 2).

According to the protocol, one retinal image centered on the macula was captured for each eye by a trained technician. Care was taken to generate gradable quality images.

All color images were evaluated with respect to the chromaticity. Images were analyzed exactly as they were outputted from the two devices. No image processing (e.g. tone and contrast enhancing/adjustment, color normalization) was performed.

Fundus cameras

System 1

The Eidon is a slit confocal system that captures 14 megapixel 60-degree retinal images in an automated fashion through a non-mydriatic pupil (as small as 2.5mm). The light source is a broad spectrum white light LED (440-650 nm).

System 2

A high-definition, non-mydriatic color fundus camera was used to acquire 45-degree 12 megapixel digital images. The system is capable of capturing images through pupils as small as 3.3 mm insize and features a xenon light source.

Chromaticity analysis

Since the two devices produce images with different angles of view, for the purpose of performing chromaticity analysis, we cropped the images in order to have the same retinal field size for evaluation (Figure 1).

The images between devices were compared in a structured color space, *i.e.* a mathematical model where each color can be represented by a set of coordinates [8,9]. Since the color of a single pixel corresponds to a position in the color space, located by its coordinates, the totality of the pixels in an image defines a region that is a subset of the whole color space. This region is distinctive for every image and thus we termed it the *color signature*.

In this study, we used the default *RGB color space* and the *rgb chromaticity color space* [10]. Whereas in the *RGB* (Red, Green, Blue) *color space* a single pixel is identified by the intensity of Red, Green, and Blue primary colors, the same pixel in the *rgb chromaticity space model* is represented by the normalization of its RGB intensities:

Due to technical limitations, equation 1 has been placed in the supplementary files section.

From now on, we will refer to the primary color intensities with uppercase letters and to their normalized values (the chromaticity) with lowercase letters. Since *rgb chromaticity* is normalized over intensities, its descriptive power is invariant to illumination and related only to the quality of the color. For example, a dark pure red represented by its primaries *RGB* = [50, 0, 0] is different than a bright pure red *RGB* = [200, 0, 0]; in the *chromaticity space*, where a color is represented by the proportions of intensities rather than by the intensities themselves, both the dark and bright pure red are expressed as *rgb* = [1, 0, 0].

By definition, the sum of *r, g, and b* will always equal one: because of this property the *b* dimension could be omitted without causing any loss in information. Thus, the *color signature* of an image can be displayed as a distribution of points in the *r and g* axes of the *chromaticity space* (Fig. 2, 3, and 4). In the *rg chromaticity space* the horizontal axis represents the *r* component, the vertical axis represent the *g* component; the third coordinate can always be inferred (*b = 1 - r - g)*. The origin *rg = [0, 0]* corresponds to the pure blue*, rg = [1, 0]* to the pure red, and *rg = [0, 1]* to the pure green; *rgb = [⍰, ⍰, ⍰]* is the location of all shades of gray (from black to white).

Outcomes

The color signature of a single image can be synthesized using three parameters, derived from the analysis of its pixels distribution on the *rgb chromaticity space*:

Due to technical limitations, equation 2 and the requisite text has been placed in the supplementary files section.

From a diagnostic point of view, a good colourful image has a high descriptive power when it is characterized by a barycenter close to the center of the chromaticity diagram (*i.e.:* rgb = [□, □, □]) and it is surrounded by a wide and continuous cloud of pixels.

In order to characterize the capability of a device to provide images with good color signatures a large series of images have to be analyzed. We devised a set of descriptors that are computed on a population of image signatures:

Due to technical limitations, equation 3 and the requisite text has been placed in the supplementary files section.

Thereafter, a good color imaging device, developed specifically for the diagnosis of retinal pathologies, is identified by an average *barycenter* located close to the center of the color space (no color dominance); a high variability of the barycenters position (different retinal conditions are represented with different color signatures); a high value of standard deviation (retina is reproduced with a collection of distant colours); and an high *NUC* percentage (the device is able to express a continuum of different colors).

Statistical analysis

After assessing the normality of the distributions, differences in chromaticity analysis outcomes and positions in the color space were evaluated using two-tailed paired t-test and multivariate paired Hotelling's T^2. A p value of <0.05 was defined as statistically significant.

Results

Confocal white LED color and flash color fundus images were obtained from 233 eyes of 181 patients. Patients' characteristics are detailed in Table 1. A wide variety of diseases were included, though over one third of eyes showed evidence of age-related macular degeneration (AMD).

A statistically significant difference in the average *barycenter* position in the chromaticity space was recorded between the two color imaging devices ($p<0.001$) (Figure 2).

The images acquired by system 1 demonstrated an average *barycenter* position (rgb = [0.448, 0.328, 0.224]) closer to the center of the chromaticity space (rgb = [□, □, □]) while system 2 provides images with a clear shift toward red at the expense of the blue and green (rgb = [0.574, 0.278, 0.148] ($p<0.001$).

The variability of the barycenter positions was higher in system 1 than in system 2 camera. Furthermore, the standard deviation values for chromaticities *r*, *g* and *b* were 0.040, 0.017 and 0.049 using the confocal white-light imaging system and 0.031, 0.020 and 0.019 using the conventional flash fundus camera.

The average variability of the distributions was higher (0.003 ± 0.007, $p<0.001$) in system 1 images compared to system 2. Specifically, the values for the for the *r*, *g* and *b* for axes were 0.036, 0.024 and 0.028, respectively, with the confocal white-light device, and 0.036, 0.020 and 0.022 using the flash camera. The NUC percentage was higher for system 1 than for system 2 (0.071% versus 0.025%, $p<0.001$).

Results of the chromaticity analysis are summarized in Table 2.

Two clinical examples are shown in Figure 3 and Figure 4.

Case 1

A 61-year-old caucasian female presented with a large pigment epithelium detachment in her left eye associated with retinal angiomatous proliferation (RAP); a retinal hemorrhage is present next to the fovea. Best corrected visual acuity was 20/50. The color analysis of the retinal image, performed with both devices, shows that system 1 provides an image with a barycenter position closer to the center of the color space compared to the same image acquired with system 2, whose barycenter is definitely moved towards the red channel. Comparing the two images, system 2 provides a color fundus picture that appears flat and reddish (Figure 3).

Case 2

A 75-year-old caucasian male presented with a diagnosis of exudative age-related macular degeneration in his right eye and a BCVA of 20/100. The chromaticity evaluation of the retinal image acquired with system 1 shows that the cluster of pixels is wider in comparison with the same image captured with system 2. Overall, a richer color content is evident in system (Figure 4).

Discussion

Diagnostic accuracy by the means of photographic documentation is highly dependent on the quality of images, because poor image quality can impair the visualization of characteristic disease features. The color characteristics are key in distinguishing different features such as hemorrhage, pigment, or lipid which may sometimes have overlapping morphologic characteristics. Thus, accurate color rendering may be vital.

The *RGB color space* and the *rgb chromaticity space* are useful abstract mathematical models for evaluating the capabilities of a digital camera to describe, classify and compare color attributes of an acquired image. A mathematical analysis of the chromaticity can also show whether different devices are able to faithfully render colors and highlight details, giving an indirect evaluation of the relative capabilities to discern pathologic signs.

The *RGB color space* is a linear color model which represents a color as a simple combination of the three primary colors (Red, Green and Blue). The *rgb chromaticity space* is derived from the *RGB color space*, and since it is normalized, it is able to describe the color content of an image independently from its intensity. It is commonly visualized as a triangle where each vertex represents a primary color, while in the centroid all colors are equally represented.

The color signature of an image is defined as the subset region of the rgb chromaticity space located by the distribution of its pixels. It represents the variety of colors composing an image.

The results of our study show that the Eidon confocal, white LED fundus camera system provides a well-balanced color image, because the barycenter position is generally located very close to the center of the *rgb chromaticity* space. By contrast, pictures acquired by a conventional flash-based fundus camera are characterized by an high predominance of red color, resulting in an over-saturated and potentially less informative retinal image.

The richness of the color content of an image is quantified by a measure of the dispersion of the pixels around its barycenter. Chromaticity analysis of our study sample showed that images acquired with Eidon offer a wider cluster of pixels in comparison with the same image captured with the conventional fundus camera. This suggests that there is a broader range or greater “richness” of color in the confocal LED image.

Another key aspect for assessing the color capability of an imaging device is the size of color gamut. The color gamut is the range of color that a device is able to display in relation to the RGB color space. The normalized chromaticity value is a measure to define the color gamut of a specific digital camera. In our study, the normalized chromaticity value is higher for the confocal LED system compared to the conventional fundus camera. This finding highlights that a conventional system provides images with a smaller color gamut in the RGB space, which means that it covers a smaller range of colors. Hence, the confocal color system is able to provide images with a wider representation of colors. This may

theoretically provide greater contrast for disease feature assessment. Contrast, or the ability to distinguish pathology from the normal background is essential to the diagnostic accuracy of a system. In color retinal imaging this attribute is based on chromaticity discrimination. Chromatic discrimination refers to the ability of an observer to distinguish two colors. It can be measured as the minimum variation needed in chromaticity to achieve a minimally noticeable difference from any point in the color space diagram. This analysis results in a MacAdam's ellipse, which is a region on a chromaticity diagram which contains all colors which are indistinguishable, to the average human eye, from the color at the center of the ellipse [11,12].

From MacAdam's studies two main conclusions can be drawn. First, given two image's signatures with the same dispersions, human vision is more sensitive to differences in the one that ranges through different colors than in the one that lies on the same tonality (barycenter located at the center of the gamut triangle vs. green and red periphery). Second, the wider the cluster of pixels surrounding the barycenter, the higher is the probability that two points of interest are located far from each other on the chromaticity diagram. Conversely, when the cluster of pixels is concentrated around the barycenter, it is more probable that the two points are located within the same MacAdam's ellipse, and thus are indistinguishable.

To further clarify these concepts, we plotted in the chromaticity diagram seven reddish points of the same retinal field captured with confocal LED system and with the flash color fundus camera. It can be easily appreciated that the reds acquired with confocal LED system are set at greater distance than those acquired with the flash color device (Figure 5). This reflects the fact that in this case the confocal system is able to make the color discrimination more noticeable for human eyes.

A final point that merits discussion is the wider variability of the barycenter position in images acquired with the confocal LED device. This finding mirrors an important characteristic of photographic instruments. In fact, when images of different fundi are captured, a device able to produce signatures with different barycenters should be considered more capable and versatile than one that always generates the same barycenter.

We may infer that the confocal LED system produces color images with a greater descriptive power compared with a traditional flash-based fundus camera, because it produces color images with a greater richness of the color content.

There are technical reasons which account for these observed differences in color rendering between the two instruments. First, the two devices use different light sources. The confocal device utilizes a white-light LED illumination while the flash color camera uses a xenon bulb light source. It is well-known that colors look different depending on the spectral characteristics of the light source. Moreover, the different on-device image processing algorithms employed in the two fundus cameras can either emphasize red and orange wavelengths over blues and greens (device 2), or produce a smoother color curve, with appropriate representation of the blue and green wavelengths (device 1). A second and critical difference is the confocal attribute of the LED system. By using a slit confocal pin-hole, light reflected from out-of-

focus layers is masked and provides only marginal contribution to image formation. This typically reduces the choroidal contribution to the red channel, which may otherwise “fog” or reduce contrast in the image.

Conclusions

In conclusion, it is well-known that color is a matter of perception and subjective interpretation. As a consequence, different subjects observing the same object, will draw upon different references and experiences and describe the exact same color with different terms. However, methods for expressing color numerically are available and can help in more objectively assessing the color attributes and capabilities of color imaging systems than subjective human assessments. Using a mathematical approach, we observed that a confocal white-light LED system can produce color images which are more balanced (i.e. not saturated by the red component) and “richer” (greater color discrimination and broader gamut) compared with traditional flash color fundus images. Although these benefits should theoretically yield greater discriminative power and diagnostic accuracy, they will need to be confirmed by prospective clinical comparison studies.

Abbreviations

AMD: age-related macular degeneration; AVG: average; BCVA: best-corrected visual acuity; cSLO: scanning laser ophthalmoscopy; DR: diabetic retinopathy; LED: Light Emitting Diode; PM: pathologic myopia; n: number; NUC: number of unique colors; RAP: retinal angiomatous proliferation; RAO: retinal artery occlusion; RGB: red-green-blue; RVO: retinal vein occlusion; SD: standard deviation; VMI: vitreomacular interface.

Declarations

Ethics approval and consent to participate

The study protocol follows the tenets of the Declaration of Helsinki and was approved by the IEMO review board. Written, informed consent was obtained from all the participants before entering the study.

Consent for publication

Written informed consent for publication of potentially identifying information and clinical images was obtained from patients included in the study.

Availability of data and materials

The datasets used and/or analyzed during the current study are available from the corresponding author upon reasonable request.

Competing interests

VS, DV, EB: The authors declare that they have no competing interests; EP: Centervue; SRS: Centervue; Heidelberg Engineering; Optos; Topcon; Zeiss Meditec; PL: Centervue; Topcon.

Funding

This research received no specific grant from any funding agency in the public, commercial, or not-for-profit sectors.

Authors' contributions

VS, DV and PL made the conception and the design of the study. VS collected and arranged the data. EP analyzed the color images and made the chromaticity diagram for each image. DV made the statistical analysis and the interpretation of data together with VS and EP. VS and DV drafted the manuscript. EB, EP, SRS and PL were contributors in editing the manuscript. All authors read and approved the final manuscript.

Acknowledgments

Not Applicable.

References

1. Jackman WT, Webster JD. On photographing the retina of the living eye. Philadelphia photographer. 1886;23:340-1.
2. Keane PA, Sadda SR. Retinal imaging in the twenty-first century. Ophthalmology. 2014;121:2489-500.
3. Bernardes R, Serranho P, Lobo C. Digital ocular fundus imaging: a review. Ophthalmologica. 2011;226:161-81.
4. Northrop RB. Noninvasive instrumentation and measurement in medical diagnosis. Boca Raton: CRC Press; 2002.

5. Graham KW, Chakravarthy U, Hogg RE, Muldrew KA, Young IS, Kee F. Identifying features of early and late age-related macular degeneration: a comparison of multicolor versus traditional color fundus photography. Retina. 2018;38:1751-8.
6. Borrelli E, Nittala MG, Abdelfattah NS, Lei J, Hariri AH, Shi Y, Fan W, Cozzi M, Sarao V, Lanzetta P, Staurenghi G, Sadda SR. Comparison of short-wavelength blue-light autofluorescence and conventional blue-light autofluorescence in geographic atrophy. Br J Ophthalmol. 2018; doi: 10.1136/bjophthalmol-2018-311849.
7. Borrelli E, Lei J, Balasubramanian S, Uji A, Cozzi M, Sarao V, Lanzetta P, Staurenghi G, Sadda SR. Green emission fluorophores in eyes with atrophic age-related macular degeneration: a colour fundus autofluorescence pilot study. Br J Ophthalmol. 2018;102:827-32.
8. Hodgman TC, French A, Westhead DR. Bioinformatics. 2nd ed. Oxford:Taylor&Francis Group; 2010.
9. Poynton C. Digital video and HD: algorithms and interfaces. 2nd ed. Waltham: Morgan Kaufmann; 2012.
10. Kakumanu P, Makrogiannis S, Bourbakis N. A survey of skin-color modeling and detection methods. Pattern recognition. 2007;40:1106-22.
11. MacAdam DL. Visual sensitivities to color differences in daylight. J Opt Soc Am. 1942;32:247–74.
12. von Kries J. Influence of adaptation on the effects produced by luminous stimuli. In: MacAdam DL. Sources of color science. Cambridge: MIT Press;1970. p.120-6

Tables

Table 1: Baseline characteristics

Eyes (n)	233
Age (mean±SD)	67.4±9.2
Female (%)	35
Normal fundus (n)	40
Retinal diseases (n)	193
AMD	88
Retinal dystrophies	25
DR	23
PM	13
VMI diseases	12
RVO	11
Central serous chorioretinopathy	6
Ocular tumors	4
RAO	4
Other Vascular Diseases	4
Retinal detachment	3

Legend: AMD: age-related macular degeneration; DR: diabetic retinopathy; PM: pathologic myopia; n: number; RAO: retinal artery occlusion; RVO: retinal vein occlusion; SD: standard deviation; VMI: vitreomacular interface.

Table 2: Results of chromaticity analysis

Chromaticity signature descriptor	Color Channel	Eidon	Topcon camera	Relative change Eidon vs Topcon camera (%)
Average barycenter (AVG)	r	0.448	0.574	-21.95
	g	0.328	0.278	18.28
	b	0.224	0.148	50.67
Average variability (AVG of SD)	r	0.036	0.036	0.55
	g	0.024	0.020	19.02
	b	0.028	0.022	28.09
Barycenter variability (SD)	r	0.040	0.031	28.55
	g	0.017	0.020	-16.57
	b	0.049	0.019	164.70
Average NUC (AVG)	%	0.071	0.025	180.96

Legend: b: blue; g: green; r: red; AVG: average; SD: standard deviation.

Figures

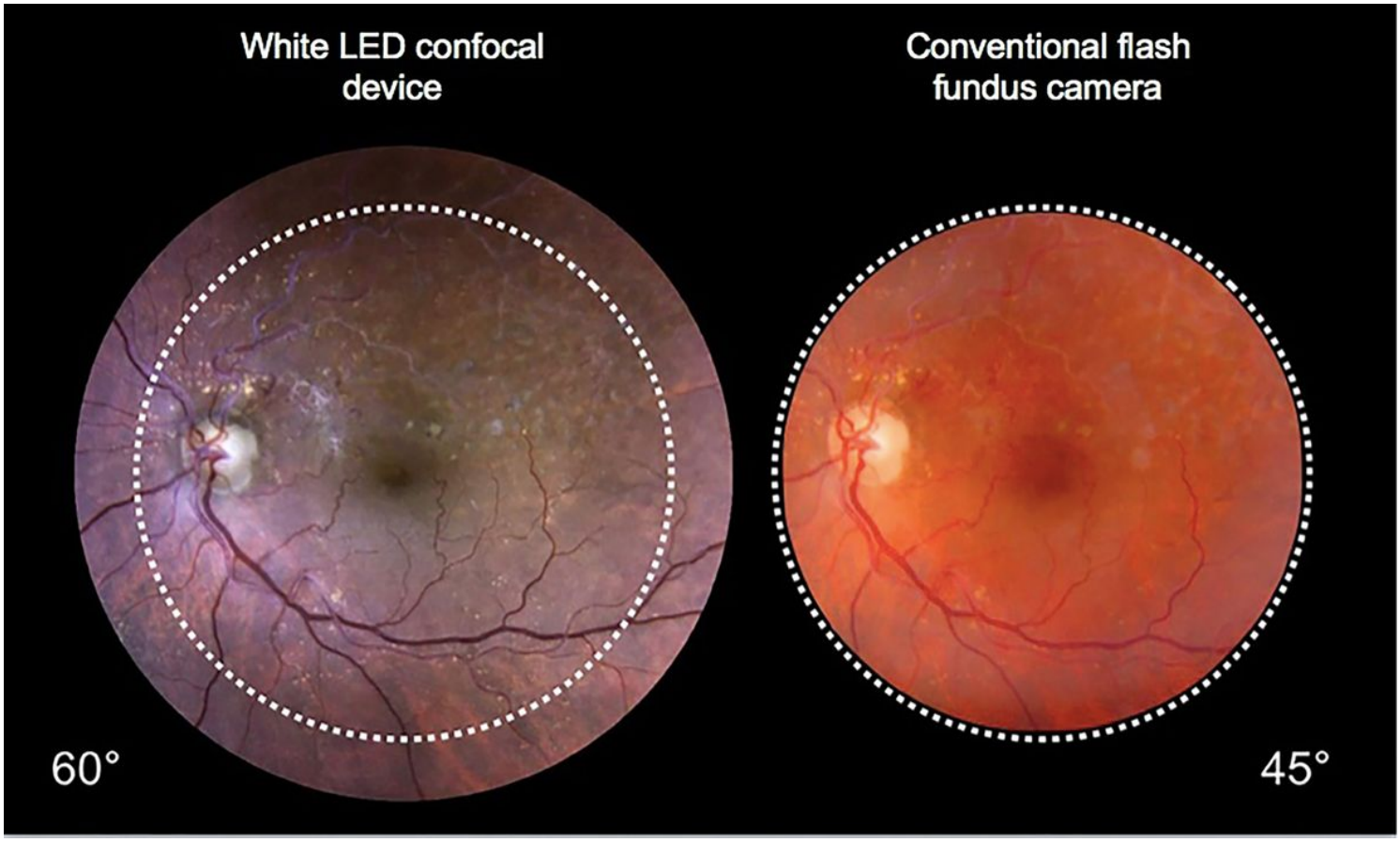

Figure 1

On the left, the image of a case of branch retinal vein occlusion acquired with confocal LED device. On the right, the image of the same patient captured with conventional fundus camera. Since both confocal LED device and the conventional fundus camera produce images with different angles of view, the images were cropped and chromaticity analysis was performed on the same retinal field size.

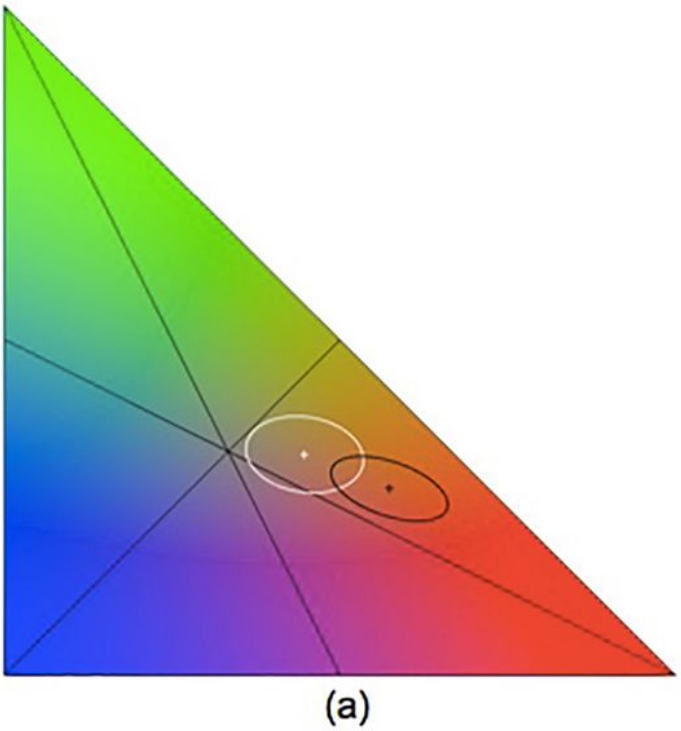

(a)

Average barycenter

Eidon:
rgb = [AVG(μ_r), AVG(μ_g), AVG(μ_b)]
= [0.448, 0.328, 0.224]
Topcon:
rgb = [AVG(μ_r), AVG(μ_g), AVG(μ_b)]
= [0.574, 0.278, 0.148]

Average variability

Eidon
rgb = [AVG(σ_r), AVG(σ_g), AVG(σ_b)]
= [0.030, 0.024, 0.028]
Topcon:
rgb = [AVG(σ_r), AVG(σ_g), AVG(σ_b)]
= [0.036, 0.020, 0.022]

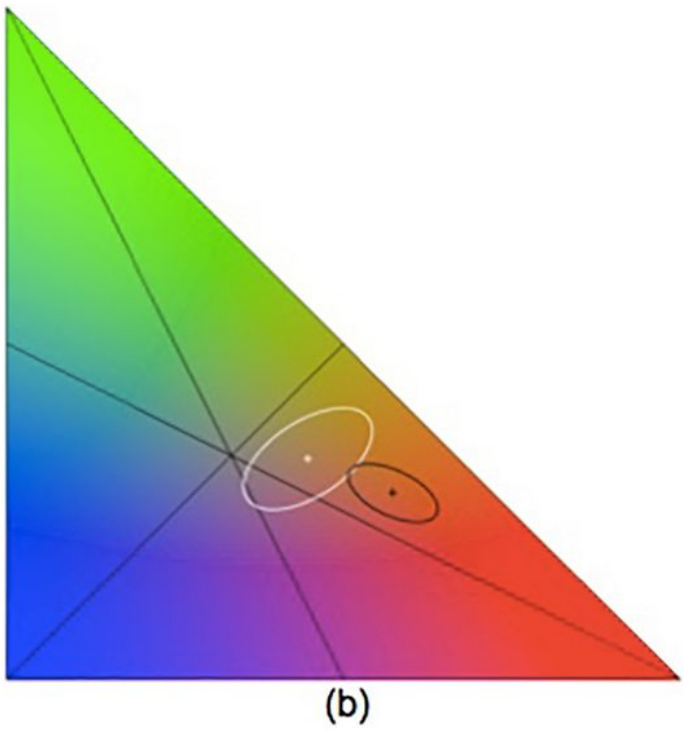

(b)

Barycenter variability

Eidon
rgb = [SD(μ_r), SD(μ_g), SD(μ_b)]
= [0.040, 0.017, 0.049]
Topcon
rgb = [SD(μ_r), SD(μ_g), SD(μ_b)]
= [0.031, 0.020, 0.019]

Figure 2

(a): the crosses are the average (AVG) position of the chromaticity barycenters for confocal LED (white) and flash color fundus (black) devices; the ellipses represent bivariate gaussian distributions with standard deviations (SD) equal to the average variability of chromaticity computed on the population of signatures; ellipses area comprise 95% of the distribution. (b): ellipses here represent bivariate gaussian

distributions with standard deviations equal to the barycenter variability computed on the population of barycenters; ellipses area comprise 95% of the distribution.

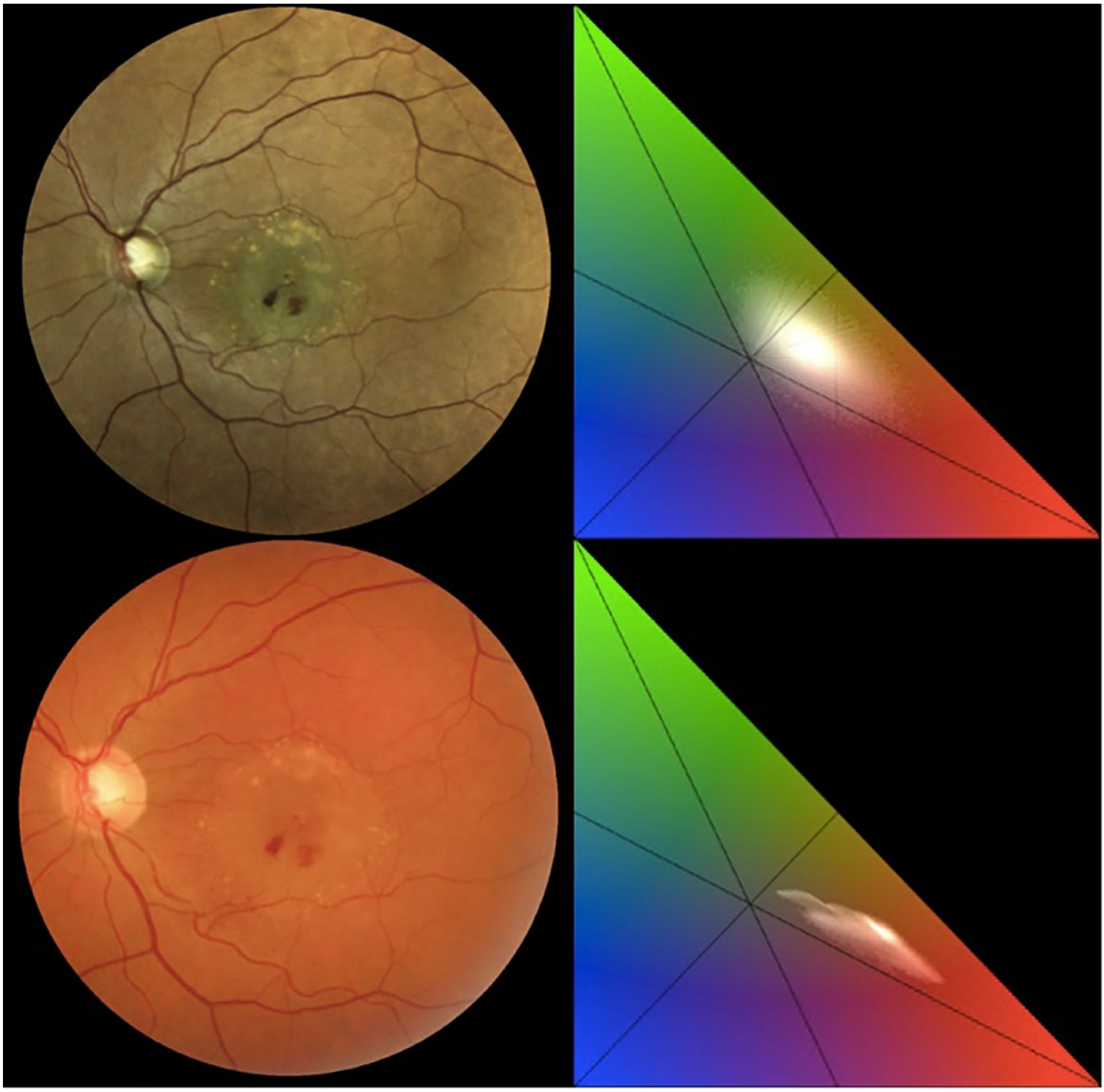

Figure 3

On the top row, the image and the chromaticity analysis of a case of retinal angiomatous proliferation acquired with the confocal LED device. On the bottom row, the image and the chromaticity analysis of the same patient captured with conventional fundus camera.

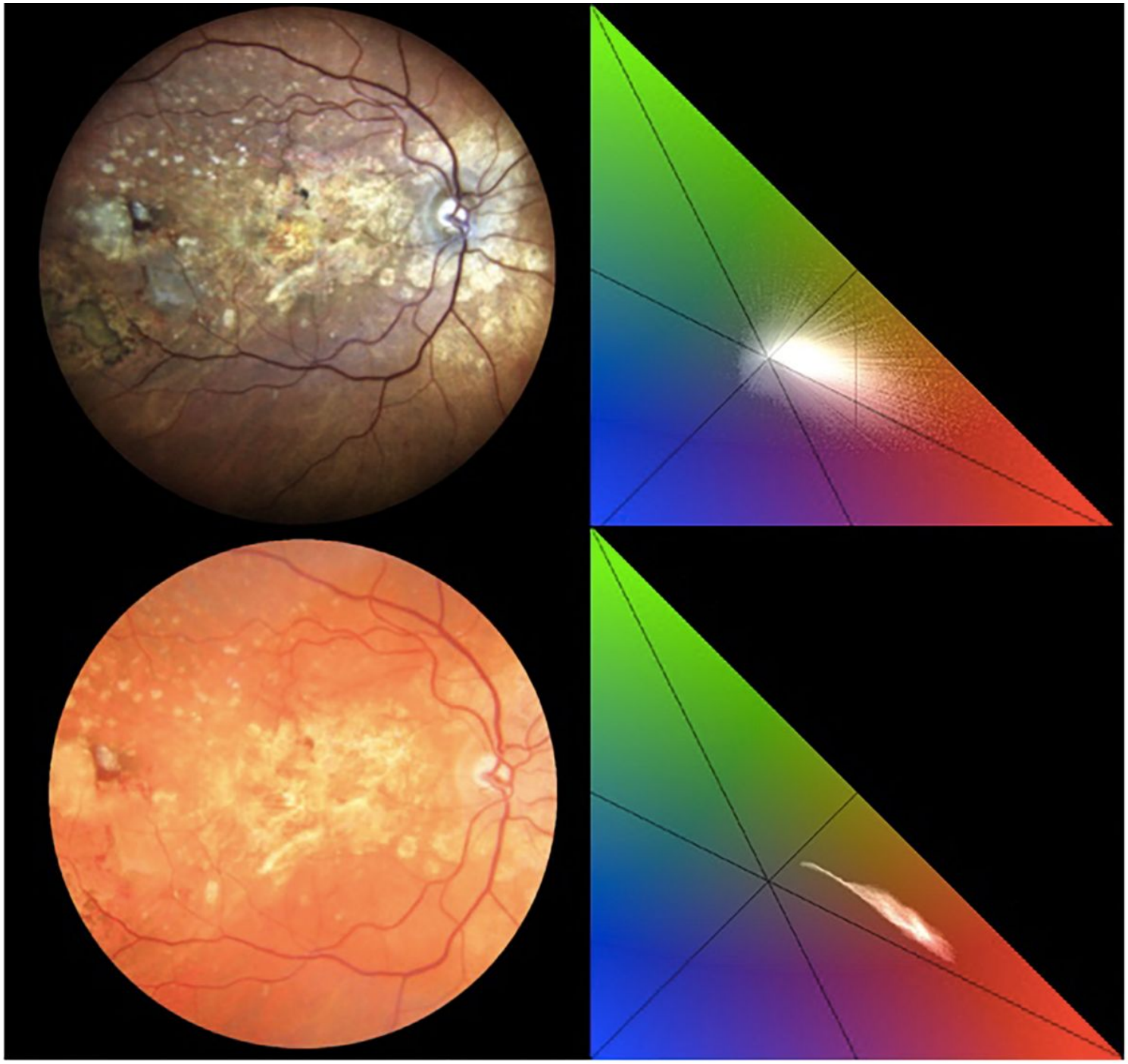

Figure 4

On the top row, the image and the chromaticity analysis of a case of exudative age-related macular degeneration acquired with confocal LED device. On the bottom row, the image and the chromaticity analysis of the same patient captured with conventional fundus camera.

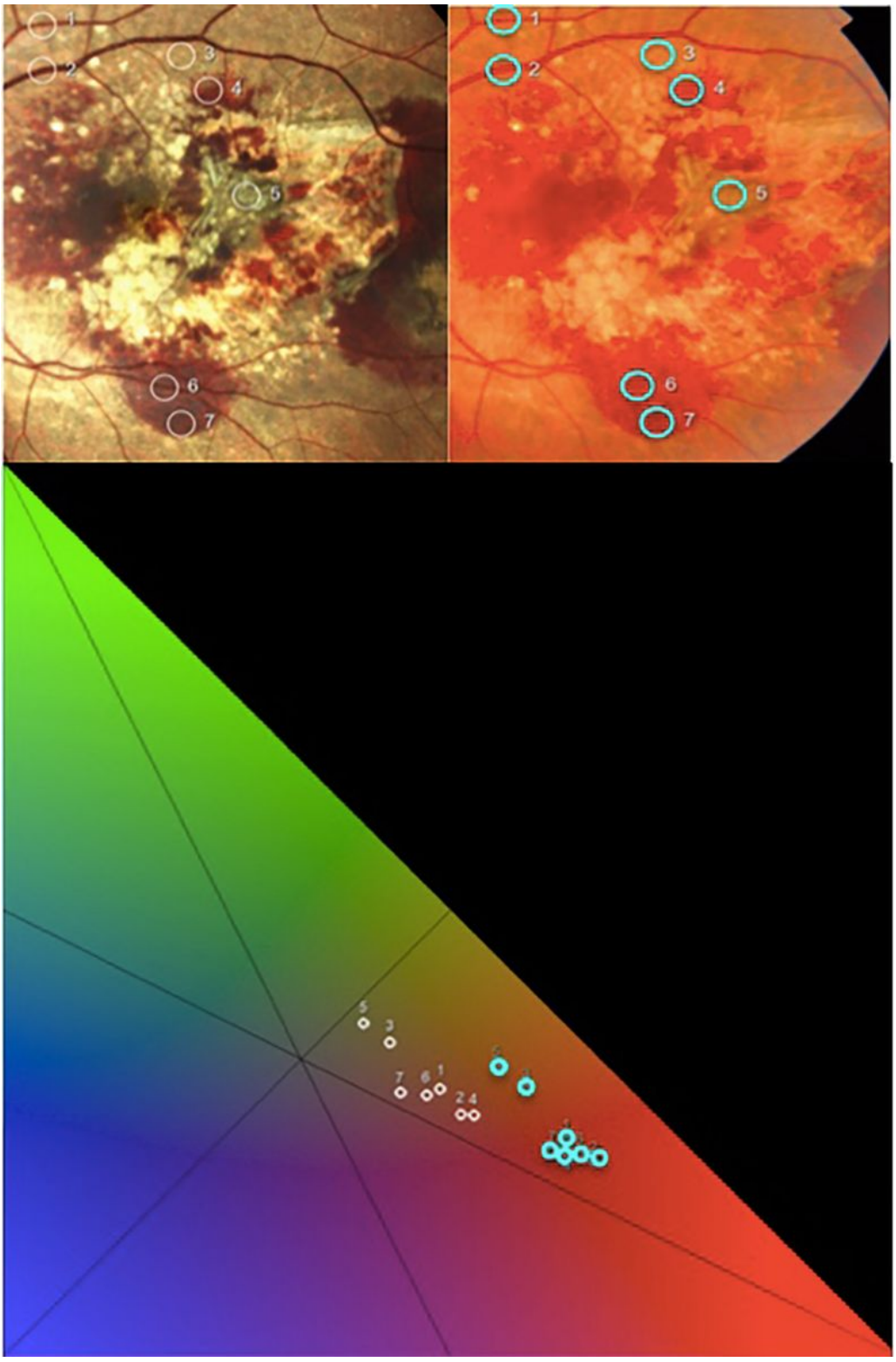

Figure 5

Seven reddish points of the same retinal field captured with confocal LED device (white rings) and with the conventional camera (light blue rings) plotted in the chromaticity diagram.

Supplementary Files

This is a list of supplementary files associated with this preprint. Click to download.

- supplement1.png
- supplement3.png
- supplement3.png